

OPEN

Hysteresis in the underdamped three-layer model

Li-Ping Jia^{1✉} & Jasmina Tekić²

The hysteretic phenomena were investigated in the three-layer model consisting of a chain of harmonically interacting atoms confined between two rigid periodical substrate potentials, where the top substrate was driven by an external force. The pinning to running and the running-to pinning transitions were examined as the driving force was varied and the influence of the equilibrium spacing and strength of the interaction of the particles in the middle layer on the static and kinetic friction force analyzed in detail. The parameter space in which the friction forces could reach their maxima or minima was determined. These results could be interesting for the selection of lubricant materials and minimization of energy loss in tribology.

More than 70 years ago, the dislocation dynamics in crystals was first described by Dehlinger with the classical one dimensional (1D) Frenkel–Kontorova (FK) model¹. Later, the FK model has been applied extensively in many problems of nonlinear physics, including: vortex lattice in Superconductivity², Josephson junctions systems³, charge or spin density waves^{4,5}, tribology^{6–9}, etc. Especially in connection with solid friction phenomena, the application of driven underdamped Frenkel–Kontorova-type model has received an increasing attention as a possible interpretative tool that provides a deep understanding of the complex field of nanotribology^{10–13}.

In the recent experimental studies, the influence of the chain stiffness on the kinetic friction force was investigated in three-layer model with incommensurate structure. According to these results, for larger chain stiffness, golden mean incommensurate structure presents a very regular periodic motion. Under the same chain stiffness, the golden mean structure has higher kinetic friction than spiral mean structure¹³. These results are useful for understanding the energy loss in nanotribology. In Ref.¹⁴, hysteresis in the two-dimensional Frenkel–Kontorova model was studied where the dependence of four critical forces on interatomic strength, winding number, misfit angle, and external driving force was examined¹⁴. In Ref.¹⁵, hysteresis was found even in overdamped one-dimensional Frenkel–Kontorova model. Hysteresis and the friction phenomena have been studied previously in two layer models^{14–16}. However, hysteresis in the underdamped three-layer model is seldom studied though in real situations, the so-called "third bodies" are often mediated between two solids, which act like a lubricant film.

In the present paper, we consider a three layer model, which consist of a driven underdamped chain of anharmonically interacting atoms confined between two periodic sinusoidal substrate potentials. Starting from the three-layer model proposed by Bruan et al. in Ref.¹³, where a chain of interacting particles is embedded between two rigid sinusoidal substrates and the top substrate is pulled through a spring connected to a stage with uniform motion, we in a way improve the model by changing the spring for a gradually increasing external driving force. We will examine the influence of the chain stiffness and equilibrium spacing for the commensurate structure on the maximum static and the maximum kinetic friction, when the top substrate is driven by the force.

Results

In Fig. 1, the variation of the upper substrate velocity v as a function of the driving force F_{ext} in the three different regimes of the equilibrium spacing b and the particle interaction strength k is presented. As the force F_{ext} increases from zero, at some value, the velocity v of the substrate potential of the upper layer is changed from zero to non-zero, we define that point as the maximum static friction F_{s1} . With the further increase of driving force the system remains in the running state. If from there we begin to reduce the driving force slowly, at some value of driving force the velocity of the upper layer droops to zero. We define this point as the kinetic friction force F_{k1} . A hysteretic phenomenon takes place in this case when $F_{s1} = F_{k1}$ (see Fig. 1). As we can see, both parameters of k and b strongly influence F_{s1} and F_{k1} . In the same way as in Fig. 1, we analyze the average velocity of the middle layer \bar{v} , which is presented as a function of the driving force F_{ext} in the three different regimes of b

¹Department of Physics, Longdong University, Qingyang 745000, China. ²Department of Theoretical and Condensed Matter Physics-020, "Vinča" Institute of Nuclear Sciences, National Institute of the Republic of Serbia, University of Belgrade, PO Box 522, 11001 Belgrade, Serbia. ✉email: pp2008634@163.com

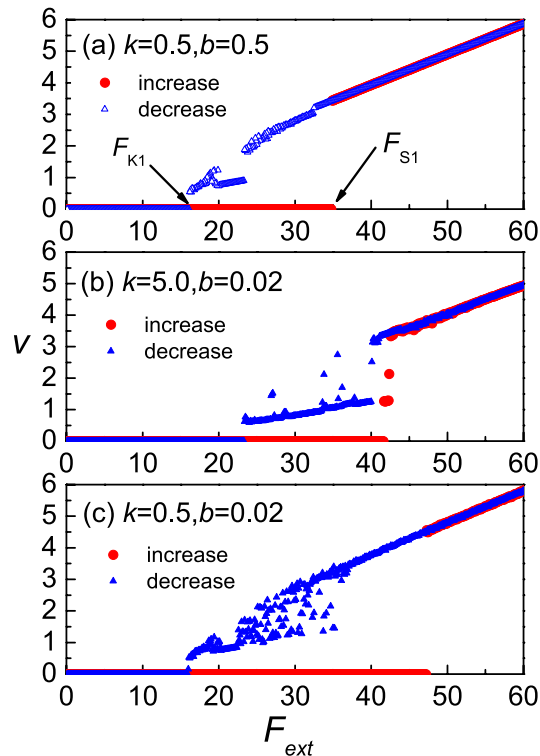


Figure 1. The upper substrate velocity v as a function of the driving force F_{ext} in different equilibrium spacing b and particle interaction strength k regimes: (a) $k = 0.5$, $b = 0.5$; (b) $k = 5.0$, $b = 0.02$; (c) $k = 0.5$, $b = 0.02$. F_{ext} is the driving force normalized to $F_{ext0} = 1\text{ N}$ and v is the upper substrate to $v_0 = \sqrt{2\pi/a} = 4.0 \times 10^{-7}\text{ m/s}$.

and k in Fig. 2. Again, we define two critical forces as: F_{s2} and F_{k2} . The hysteretic phenomenon takes place in this case when $F_{s2} = F_{k2}$ (see Fig. 2). As we can see, for the same k and b , $F_{s1} = F_{s2}$, $F_{k1} = F_{k2}$. We will consider the case of the system when $F_{s1} = F_{s2} = F_s$, and $F_{k1} = F_{k2} = F_k$. Therefore, we will only examine F_s , and F_k , which is enough to illustrate the behavior. In order to understand the hysteretic phenomenon in more detail we will examine how the system parameters affect the static and kinetic friction forces.

The dependence of the static friction F_s and the kinetic friction F_k on the external driving force F_{ext} and equilibrium spacing b for different strength k is given in Fig. 3a–f (the red line represents the static friction and the blue line represents the kinetic friction). The results show that the difference between the maximum and the minimum values of the both F_s , and F_k increases as the strength k increases. However, while the maxima of F_k increase with k , the maximum value of the static friction force, on the other hand, remains independent of the parameter k and keeps the constant value $F_s = 50$. Meanwhile, if we look at the minima, in both cases for F_s , and F_k , their values decrease as the parameter k increases. The dependence of the static friction force on the parameter b is periodic with the periodicity, which is equal 1. Nevertheless, the dependence of the kinetic friction force on the parameter b is quasi-periodic with the periodicity, which is also 1. Thus, we can consider only one period, which would be enough to analyze the behavior.

The dependence of the static friction F_s as a function of equilibrium spacing b and different strength k is presented in Fig. 4. We can see that when b is in the range of 0.1–0.4, F_s decrease as both the equilibrium spacing b and different strength k increase. When b is in the range of 0.4–0.6, F_s decrease as different strength k increase. However, when b is in the range of 0.6–1.0, F_s increases with the increase of b and decreases with the increase of k . The dependence of the kinetic friction F_k as a function of equilibrium spacing b and different strength k is presented in Fig. 5. The system has the least kinetic friction for the values of k and b , which corresponds to blue region of the plane, while when b is between 0.9 and 1.0, it has the most kinetic friction.

Discussion

In the present paper, the dynamics of an underdamped three-layer model, which consists of a harmonic chain confined between two periodical substrate potentials has been investigated. The obtained results showed that when the upper substrate was driven by the external force F_{ext} , hysteresis phenomenon would appear not only in the upper substrate but also in the middle chain. The static and kinetic friction forces for both layers have been analyzed, where the particular case when both layers had the same static and the same dynamic friction forces was considered. Their dependence on the equilibrium spacing and the strength of the interparticle interaction in the middle layer was examined in detailed and a diagram, which clearly shows the regions with the maximum

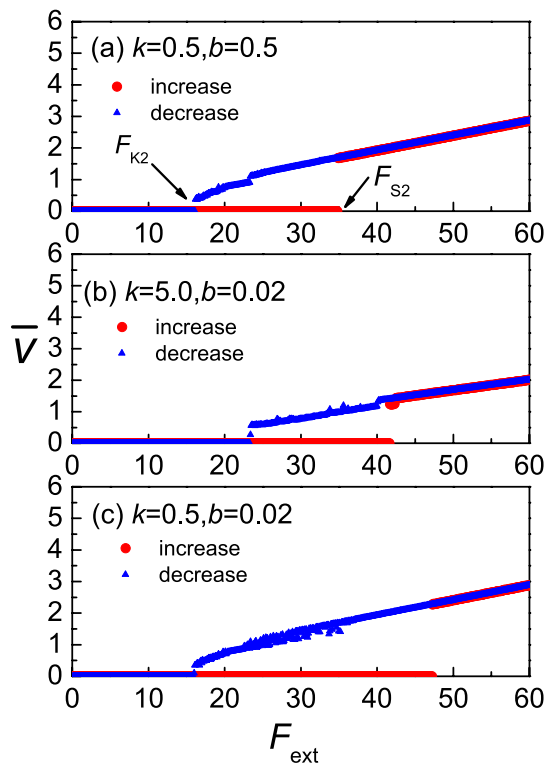


Figure 2. The average velocity of middle layer \bar{v} as a function of the driving force F_{ext} in different equilibrium spacing b and particle interaction strength k regimes: (a) $k = 0.5, b = 0.5$; (b) $k = 5.0, b = 0.02$; (c) $k = 0.5, b = 0.02$.

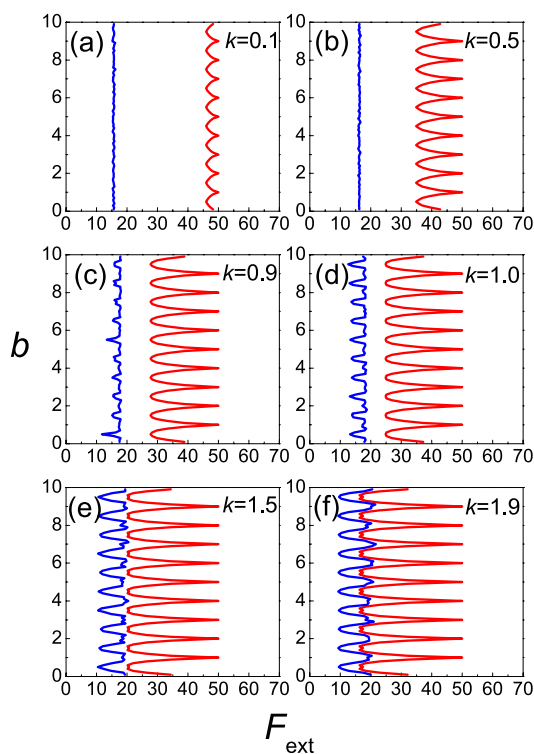


Figure 3. Contour plot of the static friction F_s and the kinetic force F_k as a function of equilibrium spacing b with different strength k : (a) $k = 0.1$; (b) $k = 0.5$; (c) $k = 0.9$; (d) $k = 1.0$; (e) $k = 1.5$; (f) $k = 1.9$. (the red line represents the static friction and the blue line represents the kinetic friction.).

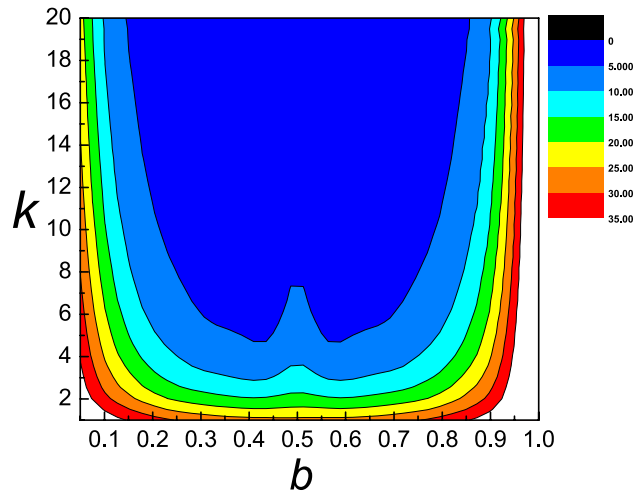


Figure 4. Contour plot of the static friction F_s as a function of equilibrium spacing b and different strength k . Different colors in the figure represent different values of the static friction.

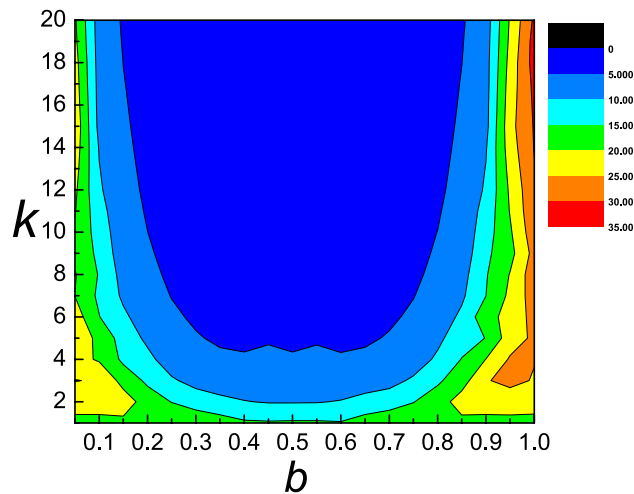


Figure 5. Contour plot of the kinetic friction F_k as a function of equilibrium spacing b and different strength k . Different colors in the figure represent different F_k values of the kinetic friction.

or minimum frictions determined. The presented results can provide reference for the selection of lubricant materials and the reduction of the energy loss in the systems.

A similar experiment can be done a graphite flake between the same crystalline surfaces (for example, iron crystal). The external driving force acts on the upper layer, but there is no driving force in the middle layer, the bottom substrate potential is fixed. In this case, the middle layer is lubricant. If the driving force is not large enough, the middle and upper layer remains motionless. If the driving force reaches a certain critical force, the upper and middle layers begin to move, the critical force is the maximum static friction. The maximum kinetic friction force has a similar definition. The parameters of lubricant determine the maximum static friction and the maximum kinetic friction force¹³.

Methods

The three-layer model consists of a chain of N harmonically interacting particles interposed between two rigid generally sinusoidal substrates as shown in Fig. 6. The top substrate (the upper layer) is driven by the force F_{ext} , and it satisfies the following equations of motions¹³:

$$M\ddot{X}_{top} = - \sum_{i=1}^N \gamma(\dot{X}_{top} - \dot{x}_i) + \sum_{i=1}^N \frac{1}{2} \left[\sin \frac{2\pi(X_{top} - x_i)}{c} \right] + F_{ext}. \tag{1}$$

The equation of motion of the i -th particle of the middle layer is given as

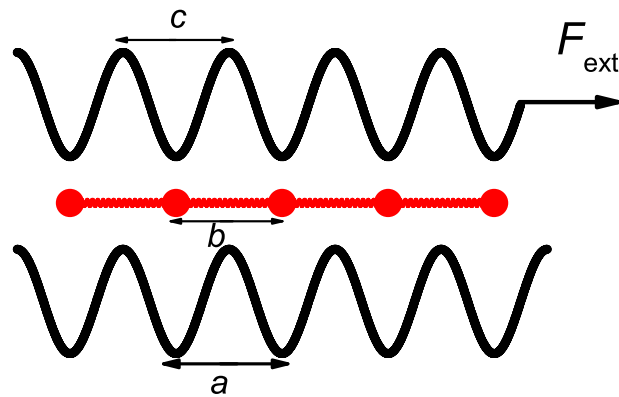


Figure 6. Schematic drawing of the underdamped three-layer model.

$$m\ddot{x}_i = -\gamma\dot{x}_i - \gamma(\dot{x}_i - \dot{X}_{top}) + \frac{d}{dx_i} \sum_{i \neq j} V(|x_i - x_j|) + \frac{1}{2} \left[\sin \frac{2\pi x_i}{a} + \sin \frac{2\pi(x_i - X_{top})}{c} \right]. \quad (2)$$

In the whole process, the lower substrate (the lower layer) has been fixed. In Eqs. (1) and (2), m and M are the mass of the particle of the middle layer and the upper substrate, while x_i ($i = 1, 2, 3 \dots N$) and X_{top} stand for their coordinates, respectively. γ is a phenomenological parameter substituting for various sources of dissipation, required to achieve a stationary state (here, we choose $\gamma = 0.2$), but otherwise with no major role in the following. $V(X)$ is the interatomic interaction potential between particles in the middle layer. We assume that it has the following harmonic form:

$$V(X) = \frac{k}{2} [(X - b)^2], \quad (3)$$

with a strength k and equilibrium spacing b . X is the difference of the coordinates between the nearest neighbors. We have used dimensionless units and consider the particles mass $m = M = 1.0$, and the equal periods of all three layers $a = c = 1.0$. The last (sinusoidal) terms in Eqs. (1) and (2) represent the on-site interaction between the particles and the substrates¹³. The sinusoidal terms in Eqs. (1) and (2) represent the on-site interaction between the particles and the substrates. The magnitudes of the rigid potentials are chosen such that the same factor (1/2) sits in front of their derivatives in the equations of motion. The Eqs. (1) and (2) have been integrated using the fourth-order Runge–Kutta method. The time step used in the simulations was 0.02τ , and a time interval of 100τ was used as a relaxation time to allow the system to reach the steady state¹³. The force was varied with the step of 10^{-4} .

The bottom substrate potential is fixed, and its damped force and force on the particles in the middle layer can be regarded as friction, which hinders the movement of the particle chain in the middle layer. In the same way, the force and damped force of the particle chain in the middle layer on the top substrate potential can also be regarded as friction, which hinders the movement of the upper layer of the bottom substrate potential, so this model can be regarded as a lubricate friction model.

Data availability

The program used in this article can be provided by the corresponding author.

Received: 13 January 2020; Accepted: 12 June 2020

Published online: 02 July 2020

References

- Kontorova, T. A. & Frenkel, Y. I. On the theory of plastic deformation and twinning I. *Zh. Eksp. Teor. Fiz.* **8**, 137–149 (1938).
- Kokubo, N., Besseling, R., Vinokur, V. M. & Kes, P. H. Mode Locking of vortex matter driven through mesoscopic channels. *Phys. Rev. Lett.* **88**, 247004. <https://doi.org/10.1103/PhysRevLett.88.247004> (2002).
- Sellier, H., Baraduc, C., Lefloch, F. & Calemczuk, R. Half integer Shapiro steps at the 0π crossover of a ferromagnetic Josephson junction. *Phys. Rev. Lett.* **92**, 257005. <https://doi.org/10.1103/PhysRevLett.95.126104> (2004).
- Thorne, R. E., Hubacek, J. S., Lyons, W. G., Lyding, J. W. & Tucker, J. R. Ac–dc interference, complete mode locking, and origin of coherent oscillations in sliding charge-density-wave systems. *Phys. Rev. B* **37**, 10055. <https://doi.org/10.1103/PhysRevB.37.10055> (1988).
- Thorne, R. E., Lyons, W. G., Lyding, J. R., Tucker, J. W. & Bardeen, J. Charge-density-wave transport in quasi-one-dimensional conductors. I. Current oscillations. *Phys. Rev. B* **35**, 6348. <https://doi.org/10.1103/PhysRevB.35.6360> (1987).
- Granato, E. & Ying, S. C. Dynamical transitions and sliding friction in the two-dimensional Frenkel–Kontorova model. *Phys. Rev. B* **57**, 7. <https://doi.org/10.1103/PhysRevB.59.5154> (1999).
- Braun, O. M. Simple model of microscopic rolling friction. *Phys. Rev. Lett.* **95**, 126104. <https://doi.org/10.1103/PhysRevLett.95.126104> (2005).
- Li, H. B., Zhao, H. & Wang, Y. H. The static properties of multi-chain Frenkel–Kontorova model: Ground state and static friction. *Phys. Lett. A* **298**, 361–368 (2002).

9. Hentschel, H., Family, F. & Braiman, Y. Friction selection in nonlinear particle arrays. *Phys. Rev. Letts.* **83**, 104. <https://doi.org/10.1103/PhysRevLett.83.104> (1999).
10. Wang, C. L., Duan, W. S., Chen, J. M. & Hong, X. R. Investigation of superlubricity in a two-dimensional Frenkel–Kontorova model with square lattice symmetry. *Appl. Phys. Lett.* **93**, 153116. <https://doi.org/10.1063/1.3003862> (2008).
11. Vanossi, A., Manini, N., Divitini, G., Santoro, G. E. & Tosatti, E. Static friction on the fly: Velocity depinning transitions of lubricants in motion. *Phys. Rev. Lett.* **99**, 056101. <https://doi.org/10.1103/PhysRevLett.99.056101> (2007).
12. Vanossi, A., Manini, N., Divitini, G., Santoro, G. E. & Tosatti, E. Exactly quantized dynamics of classical incommensurate sliders. *Phys. Rev. Lett.* **97**, 056101. <https://doi.org/10.1103/PhysRevLett.97.056101> (2006).
13. Braun, O. M., Vanossi, A. & Tosatti, E. Incommensurability of a confined system under shear. *Phys. Rev. Lett.* **95**, 026102. <https://doi.org/10.1103/PhysRevLett.95.026102> (2005).
14. Tekic, J., Botha, A. E., Mali, P. & Shukrinov, Y. M. Inertial effects in the dc+ac driven underdamped Frenkel–Kontorova model: Subharmonic steps, chaos, and hysteresis. *Phys. Rev. E* **99**, 022206. <https://doi.org/10.1103/PhysRevE.99.022206> (2019).
15. Li, R. T., Duan, W. S., Yang, Y., Wang, C. L. & Chen, J. M. Hysteresis in the pinning-depinning transition in underdamped two-dimensional Frenkel–Kontorova model. *Europhys. Lett.* **94**, 56003. <https://doi.org/10.1209/0295-5075/94/56003> (2011).
16. Braun, O. M., Bishop, A. R. & Röder, J. Hysteresis in the underdamped driven Frenkel–Kontorova model. *Phys. Rev. Lett.* **79**, 19. <https://doi.org/10.1103/PhysRevLett.79.3692> (1997).

Acknowledgements

This work is Supported by the National Natural Science Foundation of China under Grant No. 11847163, Gansu province Department of Education fund item of China under Grant No. 2020A-115 and the Doctor Science Foundation of Long Dong University under Grant No. XYBY1701. The research was partly funded by the Ministry of Education, Science and Technological Development of the Republic of Serbia.

Author contributions

L.-P.J. put forward the idea, L.-P.J. writes and debugs programs, L.-P.J. and J.T. analysed the results. All authors reviewed the manuscript.

Competing interests

The authors declare no competing interests.

Additional information

Correspondence and requests for materials should be addressed to L.-P.J.

Reprints and permissions information is available at www.nature.com/reprints.

Publisher's note Springer Nature remains neutral with regard to jurisdictional claims in published maps and institutional affiliations.



Open Access This article is licensed under a Creative Commons Attribution 4.0 International License, which permits use, sharing, adaptation, distribution and reproduction in any medium or format, as long as you give appropriate credit to the original author(s) and the source, provide a link to the Creative Commons license, and indicate if changes were made. The images or other third party material in this article are included in the article's Creative Commons license, unless indicated otherwise in a credit line to the material. If material is not included in the article's Creative Commons license and your intended use is not permitted by statutory regulation or exceeds the permitted use, you will need to obtain permission directly from the copyright holder. To view a copy of this license, visit <http://creativecommons.org/licenses/by/4.0/>.

© The Author(s) 2020